Chilean Journal of Statistics
Vol. 2, No. 2, September 2011, 69–79

Spatial Statistics and Image Modeling
Special Issue: "III SEEMI"
Research Paper

Mammography image detection processing for automatic micro-calcification recognition

Clara Quintana[1,2], Silvia Ojeda[2], Germán Tirao[1,2,*] and Mauro Valente[1,2]

[1]CONICET, Argentina
[2]Facultad de Matemática, Astronomía y Física,
Universidad Nacional de Córdoba, Córdoba, Argentina

(Received: 29 April 2011 · Accepted in final form: 06 June 2011)

Abstract

It is well known worldwide that mammography imaging proved to be the best non invasive method for breast cancer diagnosis. However, it is required to have irradiation parameters set within protocols recommendations (minimal dose delivering). This work presents a whole investigation about mammography image formation by means of validated Monte Carlo simulations along with corresponding dedicated image analysis and processing. Particulary, four different image processing methods are considered, suitably introduced and investigated according to their capability for micro-calcification detection. The obtained results suggest the feasibility of all the proposed method. Furthermore, we characterize the reliability of each one and to infer the corresponding advantages/disadvantages.

Keywords: AR-2D model · Image processing · X-ray imaging.

Mathematics Subject Classification: Primary 68U10 · Secondary 92C55.

1. Introduction

Breast cancer is the most frequent cancer in women in the world. The main established strategies for breast cancer control are based on primary prevention along with early diagnosis. In this sense, breast imaging plays an outstanding role for the screening and diagnosis of symptomatic women. Therefore, it is desirable that imaging methods should achieve high sensitivity; see Peplow and Verghese (2000). During the last decades different X-ray imaging techniques showed a significant expansion in medical applications; see Sabel and Aichinger (1996), Dilmanian et al. (2000) and Lewin et al. (2002). Conventional and digital mammographies are nowadays the most used imaging techniques for breast examination (see Arvanitis and Speller, 2009; Ducote and Molloi, 2010) as well as early breast tumour detection. Mammography units may differ by X-ray beam characteristics, breast compressing plate system and X-ray detector; see Berns et al. (2006). Breast and micro-calcification (μCa) composition material absorption properties show a strong dependence on X-ray spectrum. Furthermore, specific patient breast characteristics, lesion

*Corresponding author. Germán Tirao. Facultad de Matemática, Astronomía y Física, Universidad Nacional de Córdoba, Medina Allende y Haya de la Torre, Ciudad Universitaria (5000) Córdoba, Argentina. Email: gtirao@famaf.unc.edu.ar

ISSN: 0718-7912 (print)/ISSN: 0718-7920 (online)

http://www.soche.cl/chjs

shape and size as well as examination exposure may influence the final image quality; see Brandan and Ramírez (2006). Soft-tissue radiography techniques, like conventional or digital mammography, are still the most reliable methods for detecting breast lesions. In this sense, novel imaging methods as well as image processing techniques become continuously of great interests, due to their increasing suitability for breast cancer screening.

Radiation transport in medical imaging has been largely studied and different approaches are nowadays available for investigation in this field; see Peplow and Verghese (2000), Boone et al. (2000), Delis et al. (2007), Crotty et al. (2011) and Pacilio et al. (2011). Typical anatomical imaging techniques, like radiography, mammography and computed tomography consist mainly on a radiation source (usually conventional X-ray tubes) and a associated radiation detector, like X-ray radiographic films or more modern solid state detectors. The recorded sample/patient image can be further digitalized for appropriate image processing. In this sense, image processing constitutes a valuable tool for medical imaging.

This work presents automatic methods aimed to the evaluation of mammographic image quality based on dedicated image processing techniques and devoted to μCa detection. Automatic methods consist on finding suitable parameters to detect all the microcalcifications. In order to assess the feasibility of the proposed methods, the entire modeling system is applied to a wide range of clinical situations including different spectral characteristics, breast composition and thickness, μCa shape, size and composition. A suitable hybrid simulation code is applied to perform virtual mammographic images (see Tirao et al., 2010), which allows to introduce all the required arrangement parameters, according to typical mammographic facilities and patient tissues.

In order to allow optimal read and comprehension of this paper, its organization is as follows. Section 2 is dedicated to explain the methodology used along with general overview of different image analysis methods. Section 3 shows the obtained results and brief discussions about them. Finally, conclusions are presented in Section 4.

2. Methodology

In order to study automatic image processing methodologies aimed to μCas detection and quality assessment in breast imaging, several mammography images are simulated with different physical parameters and a set of image processing techniques dedicated to the μCa detection are implemented. The simulated images are performed by means of Monte Carlo techniques (see Tirao et al., 2010) based on the general purposes Monte Carlo main code PENELOPE; see Salvat et al. (2008). Due to its intrinsic pure stochastic characteristics, the Monte Carlo approach provides satisfactory description when performing simulations devoted to assess low enough (similar to experimental data or even negligible) statistical uncertainties. To this aim, careful preliminary investigations are performed allowing to established a suitable threshold value for the require primary showers. All presented mammographic images correspond to simulations that ensure statistic uncertainties lower than 2% for the standard deviation of relevant image parameter mean values. Once the required simulation parameters are established, all the simulations are performed on the quad-core desktop PC requiring around 30 hours per simulation.

Once simulated images are carried out, the next step consists on applying different image processing techniques, previously adapted to this aim. As mentioned, four different strategies are considered for mammography image analysis. Each one of them is preliminary studied and suitably incorporated to dedicated subroutines. Finally, the performances obtained from the application of the different image processing methods to the complete set of mammography images are carefully cross-compared in order to infer some general trends and trying to establish the suitability of each one of the image processing methods.

2.1 Simulated images

Typical mammography facility has been modelled by a dedicated and validated Monte Carlo subroutine performing absorption contrast images; see Tirao et al. (2010). This tool has been applied to investigate the dependence of image quality upon irradiation configurations according to different parameters: breast thickness and tissue composition, incident beam from a Mo anode (defined by accelerating voltage) characteristics, and compositions, shapes and sizes of μCa. Selected parameters values are taken according to typical clinical situations. A total of 54 different setup combinations are studied, each one combining different parameter values, as shown in the Table 1. In order to investigate μCa detection performance, a set of nine μCas of different shapes and sizes are included within the breast for all samples,as sketched in Figure 1.

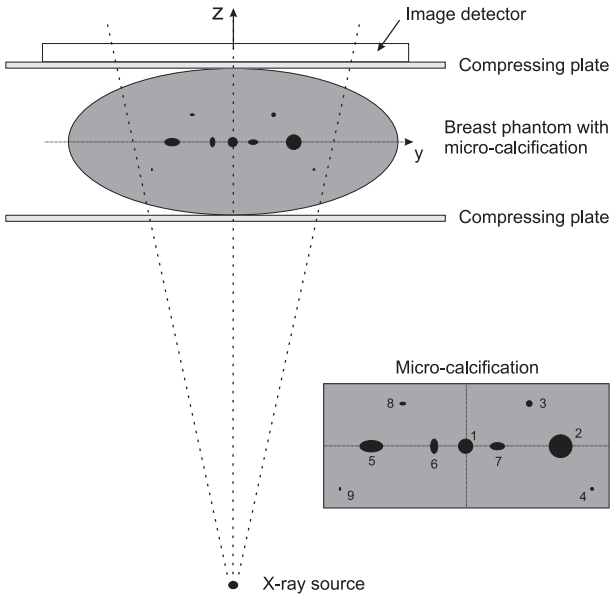

Figure 1. Simulation setup geometry to mimic a typical mammography unit. Inset: detail containing spherical (1 to 4 with radii of 2 mm, 4 mm, 1 mm and 0.5 mm, respectively) and ellipsoidal (5 to 9, with a values of 2 mm, 4 mm, 1 mm and 0.5 mm, respectively) μCa of different sizes. The ellipsoidal μCa-6 and -7 have equal size, but different orientation.

Table 1. Different configurations considered in the simulated images.

Parameter	Configuration		
Incident beam	24 kV	34 kV	40 kV
Breast thickness	30 mm	50 mm	70 mm
Breast composition	100% gandular	50% gandular - 50% adipose	100% adipose
μCa composition	calcium oxalate	calcium carbonate	

2.2 Image processing: threshold segmentation method

An image may be defined as a two-dimensional function, $f(x, y)$, where x and y are spatial (plane) coordinates, and the amplitude of f at any pair of coordinates (x, y) is called intensity or gray level of the image at that point. In many applications of image processing, pixel values belonging to the object are substantially different from those in its background. The threshold segmentation method is an enhancement technique in the spatial domain and is widely used for object detection. It consists on applying a transformation T on the intensity values of the image $f(x, y)$, resulting in a binary image $g(x, y) = T[f(x, y)]$.

The transformation T is given by Equation (1), assuming that the μCa intensities are distinguishable and lower than the background intensity

$$T = \begin{cases} 0, \text{ if } f(x,y) < \alpha, \\ 1, \text{ if } f(x,y) \geq \alpha, \end{cases} \tag{1}$$

where α is the threshold value. The α parameter would be suitably defined according to the actual situation. There are several methods, based on histogram techniques, to automatically evaluate the threshold value α, such as P-tile method (see Samopa and Asano, 2009), Gaussian mixture model (see Huang and Chau, 2008), entropy measurement (see Pal and Pal, 1989), fuzzy approaches (see Pal and Rosenfeld, 1988). In this paper, we evaluate the feasibility of finding a single threshold to detect all the micro-calcifications. For that, it is considered different thresholds with an initial value based on the average value of the image.

2.3 Image processing: edges detection

The implemented edge detection algorithm is based on the Canny (see Canny, 1986), which finds edges by looking for gradient local maxima within the original image. The gradient is calculated using the derivative of a Gaussian filter. The method incorporated two thresholds T and S, devoted to detect strong and weak edges respectively, and includes the weak edges in the output only if they are connected to strong edges. An edge in an image may point in a variety of directions; therefore, Canny algorithm uses four filters to detect horizontal, vertical and diagonal edges in the blurred image. The Canny edge detection operator returns values for the first derivative in the horizontal direction (G_x) and the vertical direction (G_y). Edge gradient module $|\overrightarrow{G}|$ and direction θ can be determined as follows:

$$|\overrightarrow{G}| = \sqrt{{G_x}^2 + {G_y}^2}, \quad \theta = \arctan\left(\frac{G_x}{G_y}\right).$$

Finally, once estimations to the image gradients are already given, a search can be then carried out to determine if the gradient magnitude assumes a local maximum in the gradient direction; see Pajares and De la Cruz (2008). In view of the absorption contrast differences between breast tissue and μCa, the application of the edge detection algorithm, based on the Canny method, may be suitable for automatic image features (μCa) detection.

2.4 Image processing: template matching routine

The template matching routine is a processing technique developed to search in the image a user-defined template of a size much smaller than the image. The matching process moves the template image to all possible positions in a larger source image and computes a numerical index (Normalized Cross Correlation) that indicates how well the template matches the image in that position. The normalized cross correlation (NCC) is taken as a likelihood measurement between the images and defined as

$$\mathrm{NCC}(f,t) = \frac{\sum_{x,y}(f(x,y) - f_{\mathrm{mean}})(t(x,y) - t_{\mathrm{mean}})}{\sqrt{\sum_{x,y}(f(x,y) - f_{\mathrm{mean}})^2 (t(x,y) - t_{\mathrm{mean}})^2}}.$$

where f represents the image, t the template, t_{mean} is the mean of the template and f_{mean} is the mean of the image in the region under the template; see Lewis (1995).

This routine generates a resulting image whose pixel intensity represents the normalized cross correlation between the image and the template in the pixel position. Therefore, it is expected to obtain higher intensity values in correspondence to maximum likelihood (correlation) between the processed image and the template.

2.5 Image processing: AR-2D segmentation

This mathematical processing method is based on the suitable and original algorithm proposed by Ojeda et al. (2010), focused on segmentation and edge detection of texture images. This method consists on locally fitting a two-dimensional autoregressive model (AR-2D) to the image. That is, the original image is divided into small regions and an AR-2D model is fitted to each of these regions. A new image is generated, putting together all images generated by fitting the local AR-2D models to the original one. Then, the autoregressive residual image is computed. As a result, the original borders are highlighted and the areas with different textures are noticed.

The first step is to obtain a new image from the original, with mean zero, i.e.,

$$g(x,y) = f(x,y) - \overline{f},$$

where $f(x,y)$ is the original image and $\overline{f}$ is the mean value of image $f(x,y)$. The next step consists establishing a moving window devoted to dividing the image $g(x,y)$ into small regions and after that a suitable AR-2D model is fitted to each of these regions (sub-images). A new image is generated, putting together all sub-images generated by fitting the local AR- 2D models to the $g(x,y)$

$$\widehat{g}(x,y) = \hat{\phi}_1 g(x-1,y) + \hat{\phi}_2 g(x,y-1),$$

where $\hat{\phi}_1$ and $\hat{\phi}_2$ are the least square estimators of ϕ_1 and ϕ_2, respectively. ϕ_1 and ϕ_2 are the parameters of the AR-2D model, based on the fact that it is possible to represent any image as

$$X(x,y) = \phi_1 X(x-1,y) + \phi_2 X(x,y-1) + \epsilon(x,y),$$

where $\epsilon(x,y)$ is a sequence of iid random variables with $\mathrm{Var}(\epsilon(x,y)) = \sigma^2$; see Bustos et al. (2009). Then, the approximated image $\widehat{f}(x,y)$ of the original image $f(x,y)$ is given by

$$\widehat{f}(x,y) = \widehat{g}(x,y) + \overline{f},$$

where $\widehat{g}(x,y)$ is the approximated image of $g(x,y)$. Finally, the autoregressive residual image $r(x,y)$ is computed as $r(x,y) = f(x,y) - \widehat{f}(x,y)$. As a result, edges within the original image are significantly highlighted and regions with different textures are noticed. One remarkable and valuable advantage of this algorithm arises from its simplicity, since it may be automatically applied.

3. Results and Discussion

In order to evaluate the performance of the considered image processing technique according to their capability of μCa detection, all the implemented method are applied on the whole set of simulated mammographic images. A qualitative quality assessment will be associated with the performance of each method.

3.1 Threshold segmentation method

Considering that the modelled breast samples have different absorption paths at each scanning position, due to the non uniform (ellipsoidal) shapes, it results that that the threshold segmentation method could not provide a satisfactory performance because of the strong limitations associated with non uniform background. Therefore, its suitability is strongly dependent on the image position, as indicated in Figure 2. As expected, it is found that the performance of this method showed significant dependence upon the threshold value and therefore requiring specific threshold values at each location of interest. Figure 2 shows that the segmentation method with the threshold A detect the 7 central μCa but it fails detecting μCa located far away from the breast central region (lower size μCa), whereas for the threshold B, the method is able to detect μCa located far away from breast central region. However, it is demonstrated that a significant loss of information at the central region arises as consequence of improving detection of remote μCa. Therefore, it seems that when considering this type of mammographic image it could not be possible to detect all the μCa through a unique segmentation threshold value. However, it should be mentioned that this drawback may be overcame if a suitable background (BG) is first subtracted from the original image. This is accomplished approximating the BG by a function obtained from the smoothing of the original image considering intensity averages along the direction transversal direction (normal to the axis around which μCas where positioned), as shown in Figure 2.

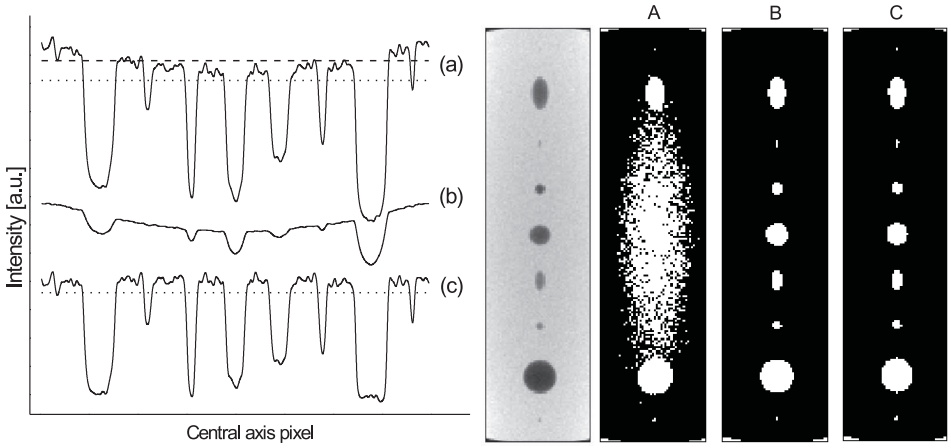

Figure 2. Micro-calcification detection using threshold segmentation method. Left side: intensity profiles of central axis where μCas are positioned. (a) original intensity profile (—), threshold A (- - -), threshold B (· · ·). (b) BG subtracted (—). (c) intensity profile without BG (—), threshold C (· · ·). Right side: from left to right: simulated mammographic image (configuration: 30 mm thick of 100% glandular breast tissue, and Mo-40 kV incident spectrum, calcium oxalate μCa composition), processing image with threshold values A, B and C respectively.

According to the resulting configuration with almost uniform background, a unique threshold value is capable of detecting central as well as remote located μCas. Therefore, incorporating suitable modifications, this method showed to be able to detect all the 9 μCas. It should be mentioned that the performances of this method when applied to the different mammography images did not show significant dependence on simulation parameters. Therefore, it does not seem to constitute a suitable criterion for assessing image quality.

3.2 Edges detection

The implemented edge detection method required to assess suitable combination of the user-defined threshold values in order to achieve a good performance. As expected, lower values for the S threshold parameter (focused on weak edges detection) resulted in a best performance in detecting image details, but becoming also higher the possibility of computing 'false positives' due to the detection of noise as image detail. Therefore, it may be advisable to overcome this risk considering high T threshold values (dedicated to strong edges detection), as reported in Figure 3. On the other hand, grater S values it may be advisable to employ lower T in order to be able to detect μCa edges, as reported in Figure 3. Therefore, the best threshold values combination may differ from image to image, which may require a preliminary study devoted to attempt the optimal parameter selection. The performed preliminary study for the cases presented in this work found that the optimal combination corresponds to $S = 0.1$ and $T = 0.1$ as is shown in Figure 3. The final performance of this method based on studies corresponding to a large quantity of threshold values combination indicated that it is able to detect 8 of the total 9 μCas.

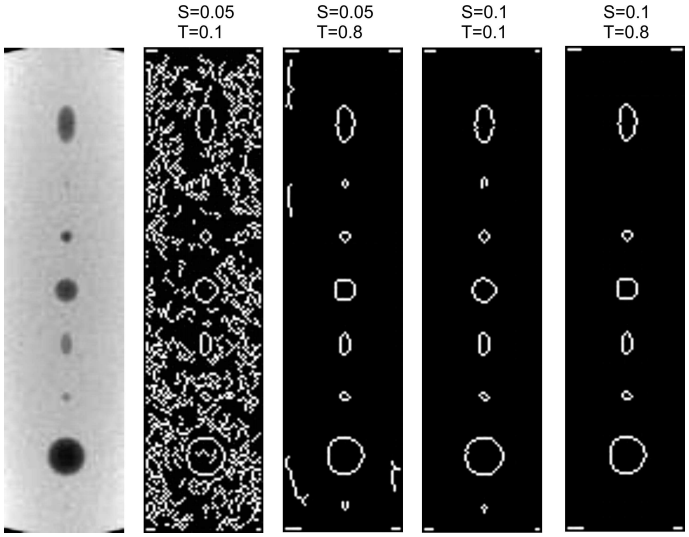

Figure 3. Micro-calcification detection using edge detection method. From left to right: simulated mammographic image (configuration: 30 mm thick of 100% glandular breast tissue, and Mo-40 kV incident spectrum, calcium oxalate μCa composition); processing image with different combination of S and T threshold values.

From the analysis of the obtained performance of this method, it can be demonstrated that it does not offer strong dependence on simulation parameters for the different mammography images. Therefore does not seem to be a suitable method for assessing image quality.

3.3 Template matching routine

The template matching routine is implemented by means of considering different binary templates. The selected pattern templates are defined using one circle of different sizes located at the center of an homogeneous background. Each template is used to search μCa within mammography sample images. The implemented technique consisted on generating maximum correlation at μCa locations if the pattern template matched the μCa size, as reported in Figure 4. Therefore, this routine has proved to be a valuable method for μCa detection, giving both information on the location and the size of the detail (μCa). Moreover, it is found that the proposed method is also capable of detecting μCa even when considering patter templates and image details of different shapes. This features requires specific and dedicated attention, due to the fact that it may constitute valuable advantages but it may also provide false positives.

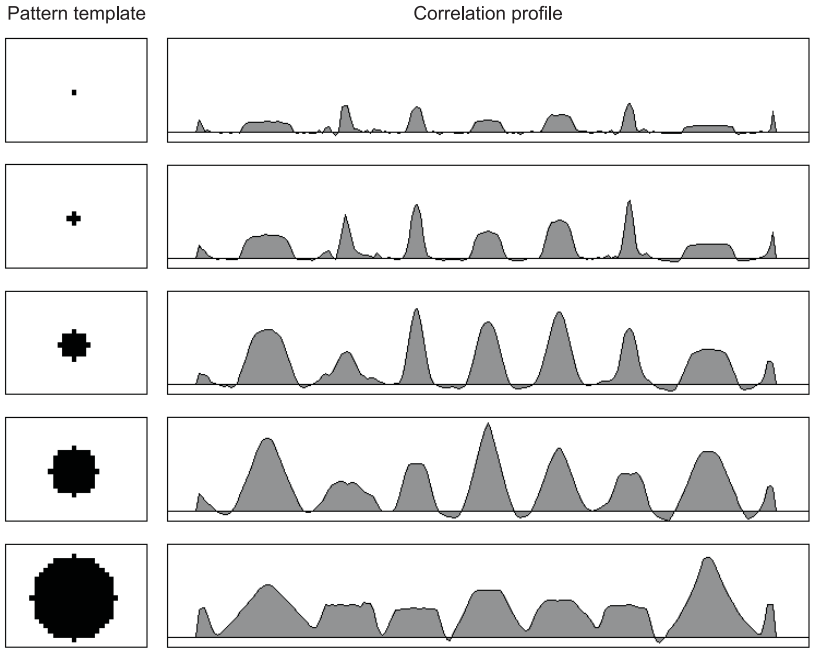

Figure 4. Micro-calcification detection using template matching routing with different template sizes. Left: pattern template. Right: corresponding central axis intensity profiles of Normalized Cross Correlation images.

Unlike previous methods, it is observed that the correlation value reflected a strong dependency on different simulation parameters, which suggest that this method may be suitable and useful for assessing somehow image quality description. Starting from predefined pattern template containing shapes similar to that of the μCa of interest, it becomes straightforward to calculate the correlation between original image and pattern template at the corresponding location and therefore obtaining very interesting and promising results regarding detail detection. In fact, higher correlation is found in absolute accordance with images having a priori better quality. Figure 5 reports the correlation value of the central μCa for a set of simulated image. It can be noticed that the obtained correlation values reflect the same tendency as the expected quality according to the different parameters of each mammographic images. In this sense, it may be concluded that the template matching routine has preliminary shown to be a valuable method for μCa detection and mammographic image quality evaluation.

3.4 AR-2D segmentation

Finally, the Ojeda's algorithm is tested; see Ojeda et al. (2010). The autoregressive residual images are computed for all the mammographic images. The implementation of Ojeda's algorithm for the purposes of the present work is performed selecting the moving window size exactly as the original image size in order to enhance the deviations from the original textures, mainly located at the borders. According to the model, a small window size is associated to a large number of AR model fitted to the original image. This produces a better local approximation and hence the patterns in the fitted image are very well represented. Therefore, the residual autoregressive image will not highlight the original borders and boundaries because both images are too similar.

The obtained results indicated that edges of μCas in the original image are satisfactory enhanced, which contributed to μCa detection recognizing 6 of the 9 μCas, as shown in Figure 6. The smaller details are not detected as a consequence of that the resulting information, is determined from the density of white and black pixels, and in a small region the provided information is scarce.

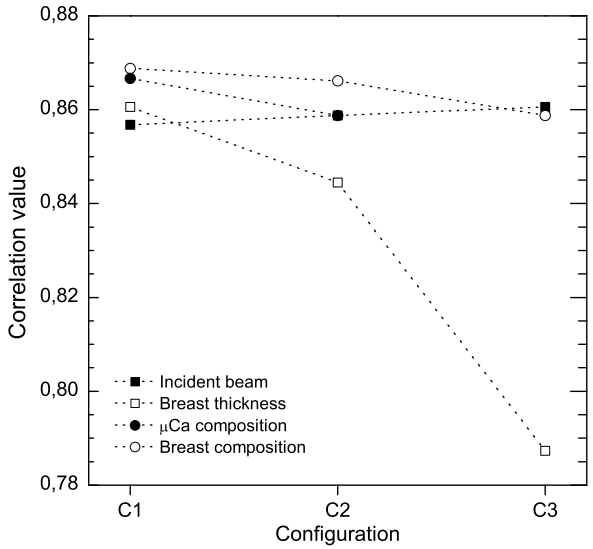

Figure 5. Correlation value of the central micro-calcification for a set of simulated image.

Besides, it is possible to noticed that there is a pre-defined direction in the mathematical processing, which it can be chosen according to convenience of particular situation. On the other hand, depending on the case, it could be possible to apply the AR-2D processing in many directions, with an extra mathematical treatment to join the results, in order to obtain a global information.

However, on the other hand, the obtained performance of this method did not present sensitivity enough for considering it as a suitable candidate for assessing image quality. Therefore, AR-2D segmentation method demonstrated to be a useful tool for micro-calcification detection but it does not constitute a suitable method to image quality assessment.

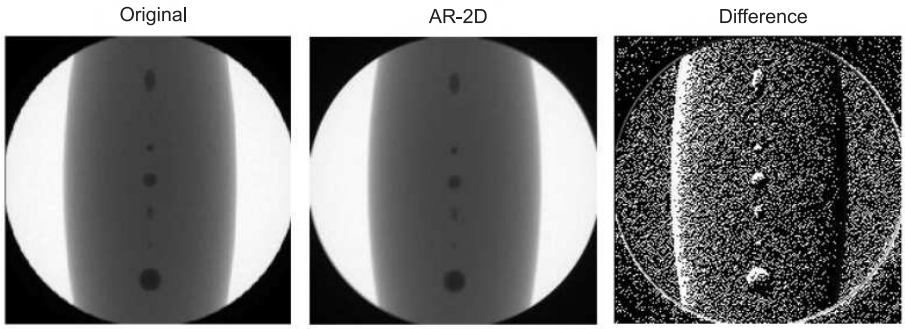

Figure 6. AR-2D segmentation technique in simulated mammographic image (configuration: 30 mm thick of 100% glandular breast tissue, and Mo-40 kV incident spectrum, calcium oxalate μCa composition).

4. Conclusions

A suitable set of mammographic images has been successfully achieved using a validated simulation tools; see Tirao et al. (2010). This set of images considered wide ranges of variation for the breast imaging relevant parameters in order to include all typical clinical situations. Therefore, the obtained results from further image processing may constitute an acceptable representation of real situations. With the aim of assessing automatically evaluation the effects on mammography image due to the different irradiation parameters, it has been proposed to consider suitable implementation of different mechanisms for image processing. In this sense, different mammography image processing techniques have been proposed and investigated. Therefore, their reliability and suitability for automatic detail detection could be assessed as well as carefully studied. As a first approach, main interests are focused on μCas detection and, when possible, image quality assessment. As preliminary demonstrated, the –background subtracted– threshold segmentation, the edge detection filter and the AR-2D segmentation methods have proved to be valuable tools for automatic micro-calcification detections, but they do not seem to be suitable for image quality assessment. On the other hand, the template matching routine has shown to be able for micro-calcification detection and furthermore it demonstrated to be a useful tool to image quality evaluation.

Acknowledgements

Authors are grateful to SeCyT – Universidad Nacional de Córdoba for partially supporting this project, as well as CONICET, Argentina.

References

Arvanitis, C.D., Speller, R. 2009. Quantitative contrast-enhanced mammography for contrast medium kinetics studies. Physics in Medicine and Biology, 54, 6041-6064.

Berns, E.A., Hendrick, R.E., Solari, M., Barke, L., Reddy, D., Wolfman, J., Segal, L., DeLeon, P., Benjamin, S., Willis, L. 2006. Digital and screen-film mammography: comparison of image acquisition and interpretation times. American Journal of Roentgenology, 187, 38-41.

Boone, J.M., Lindorfs, K.K., Cooper III, V.N., Seibert, J.A. 2000. Scatter/primary in mammography: Monte Carlo validation. Medical Physics, 27, 1818-1831.

Brandan, M.E., Ramírez, V. 2006. Evaluation of dual-energy subtraction of digital mammography images under conditions found in a commercial unit. Physics in Medicine and Biology, 51, 2307-2320.

Bustos, O., Ojeda, S., Vallejos, R. 2009. Spatial ARMA models and its applications to image filtering. Brazilian Journal of Probability and Statistics, 23, 141-165.

Canny, J. 1986. A computational approach to edge detection source. IEEE Transactions on Pattern Analysis and Machine Intelligence, 8, 679-698.

Crotty, D., Brady, S., Jackson, D., Toncheva, G., Anderson, C., Yoshizumi, T., Tornai, M. 2011. Evaluation of the absorbed dose to the breast using radiochromic film in a dedicated CT mammotomography system employing a quasi-monochromatic X-ray beam. Medical Physics, 38, 3232-3245.

Delis, H., Spyrou, G., Costaridou, L., Tzanakos, G., Panayiotakis, G. 2007. Evaluating the figure of merit in mammography utilizing Monte Carlo simulation. Nuclear Instruments and Methods in Physics Research A, 580, 493-496.

Dilmanian, F.A., Zhong, Z., Ren, B., Wu, X.Y., Chapman, L.D., Orion, I., Thomlinson, W.C. 2000. Computed tomography of X-ray index of refraction using the diffraction enhanced imaging method. Physics in Medicine and Biology, 45, 933-946.

Ducote, J.L., Molloi, S. 2010. Scatter correction in digital mammography based on image deconvolution. Physics in Medicine and Biology, 55, 1295-1309.

Huang, Z.K., Chau, K.W. 2008. A new image thresholding method based on Gaussian mixture model. Applied Mathematics and Computation, 205, 899-907.

Lewin, J.M., D'Orsi, C.J., Hendrick R.E., Moss, L.J., Isaacs, P.K., Karellas, A., Cutter, G.R. 2002. Clinical comparison of full field digital mammography and screen-mammography for detection of breast cancer. American Journal of Roentgenology, 179, 671-677.

Lewis, J.P. 1995. Fast template matching, vision interface. Canadian Image Processing and Pattern Recognition Society, 95, 120-123.

Ojeda, S., Vallejos, R., Bustos, O. 2010. A new image segmentation algorithm with applications to image inpainting. Computational Statistics and Data Analysis, 54, 2082-2093.

Pacilio, M., Basile, C., Shcherbinin, S., Caselli, F., Ventroni, G., Aragno, D., Mango, L., Santini, E. 2011. An innovative iterative thresholding algorithm for tumour segmentation and volumetric quantification on SPECT images: Monte Carlo-based methodology and validation. Medical Physics, 38, 3050-3061.

Pajares, M.G., De la Cruz, J.M.G. 2008. Visión por Computador: Imágenes Digitales y Aplicaciones. Alfaomega, Mexico.

Pal, N.R., Pal, S.K. 1989. Entropic thresholding. Signal Processing, 16, 97-108.

Pal, S.K., Rosenfeld, A. 1988. Image enhancement and thresholding by optimization of fuzzy compactness. Pattern Recognition Letters, 7, 77-86.

Peplow, D.E., Verghese, K. 2000. Digital mammography image simulation using Monte Carlo. Medical Physics, 27, 568-579.

Sabel, M., Aichinger, H. 1996. Review: recent developments in breast imaging. Physics in Medicine and Biology, 41, 315-368.

Salvat, F., Fernández-Varea, J., Sempau, J. 2008. PENELOPE Version 2008. NEA, France.

Samopa, F., Asano, A. 2009. Hybrid image thresholding method using edge detection. International Journal of Computer Science and Network Security, 9, 292-299.

Tirao, G., Quintana, C., Malano, F., Valente, M. 2010. X-ray spectra by means of Monte Carlo simulations for imaging applications. X Ray Spectrometry, 39, 376-383.